The status of the Virgo gravitational wave detector

F. Acernese[6], P. Amico[10], M. Alshourbagy[11], F. Antonucci [12], S. Aoudia[7], P. Astone[12], S. Avino[6], D. Babusci[4], G. Ballardin[2], F. Barone[6], L. Barsotti[11], M. Barsuglia[8] , F. Beauville[1], S. Bigotta[11], S. Birindelli[11], M.A. Bizouard[8], C. Boccara[9], F. Bondu[7], L. Bosi[10], C. Bradaschia[11], S. Braccini[11], A. Brillet[7], V. Brisson[8], L. Brocco[12], D. Buskulic[1], E. Calloni[6], E. Campagna[3], F. Carbognani[2], F. Cavalier[8], R. Cavalieri[2], G. Cella[11], E. Cesarini[3], E. Chassande-Mottin[7], N. Christensen[2], C. Corda[11], A. Corsi[12], F. Cottone[10], A.-C. Clapson[8], F. Cleva[7], J.-P. Coulon[7], E. Cuoco[2], A. Dari[10], V. Dattilo[2], M. Davier[8], M. del Prete[2], R. De Rosa[6], L. Di Fiore[6], A. Di Virgilio[11], B. Dujardin[7], A. Eleuteri[6], I. Ferrante[11], F. Fidecaro[11], I. Fiori[11], R. Flaminio[1,2], J.-D. Fournier[7], S. Frasca[12], F. Frasconi[2,11], L. Gammaitoni[10], F. Garufi[6], E. Genin[2], A. Gennai[11], A. Giazotto[11], G. Giordano[4], L. Giordano[6], R. Gouaty[1], D. Grosjean[1], G. Guidi[3], S. Hebri[2], H. Heitmann[7], P. Hello[8], S. Karkar[1], S. Kreckelbergh[8], P. La Penna[2], M. Laval[7], N. Leroy[8], N. Letendre[1], B. Lopez[2], Lorenzini[3], V. Loriette[9], G. Losurdo[3], J.-M. Mackowski[5], E. Majorana[12], C. N. Man[7], M. Mantovani[11], F. Marchesoni[10], F. Marion[1], J. Marque[2], F. Martelli[3], A. Masserot[1], M. Mazzoni[3], L. Milano[6], F. Menzinger[2], C. Moins[2], J. Moreau[9], N. Morgado[5], B. Mours[1], F. Nocera[2], C. Palomba[12], F. Paoletti[2,11], S. Pardi[6], A. Pasqualetti[2], R. Passaquieti[11], D. Passuello[11], B. Perniola[3], F. Piergiovanni[3], L. Pinard[5], R. Poggiani[11], M. Punturo[10], P. Puppo[12], K. Qipiani[6], P. Rapagnani[12], V. Reita[9], A. Remillieux[5], F. Ricci[12], I. Ricciardi[6], P. Ruggi[2], G. Russo[6], S. Solimeno[6], A. Spallicci[7], R. Stanga[3], M. Tarallo[11], M. Tonelli[11], A. Toncelli[11], E. Tournefier[1], F. Travasso[10], C. Tremola[11], G. Vajente[11], D. Verkindt[1], F. Vetrano[3], A. Viceré[3], J.-Y. Vinet[7], H. Vocca[10] and M. Yvert[1]

[1] *Laboratoire d'Annecy-le-Vieux de Physique des Particules (LAPP), IN2P3/CNRS, Université de Savoie, Annecy-le-Vieux, France;*
[2] *European Gravitational Observatory (EGO), Cascina, Italia;*
[3] *INFN, Sezione di Firenze/Urbino, Sesto Fiorentino, and/or Università di Firenze, and/or Università di Urbino, Italia;*
[4] *INFN, Laboratori Nazionali di Frascati, Frascati (Rm), Italia;*
[5] *LMA, Villeurbanne, Lyon, France;*
[6] *INFN, sezione di Napoli and/or Università di Napoli "Federico II" Complesso Universitario di Monte S.Angelo, and/or Università di Salerno, Fisciano, Italia;*
[7] *Departement Artemis – Observatoire de la Côte d'Azur, Nice, France;*
[8] *Laboratoire de l'Accélérateur Linéaire (LAL), IN2P3/CNRS Université de Paris-Sud, Orsay, France;*
[9] *ESPCI, Paris, France;*
[10] *INFN, Sezione di Perugia and/or Università di Perugia, Perugia, Italia;*
[11] *INFN, Sezione di Pisa and/or Università di Pisa, Pisa, Italia;*
[12] *INFN, Sezione di Roma and/or Università "La Sapienza", Roma, Italia.*

We present the status of the Virgo detector which is approaching its nominal sensitivity to detect gravitational waves predicted by the General Relativity. The commissioning of Virgo in its final configuration started in 2003. The recent progress performed on the detector are detailed. We report also on the different data analysis activities carried out by the groups of the Virgo Collaboration. We briefly mention the short term planning of the Virgo commissioning and conclude this article with the different research and development programs to improve the sensitivity of the Virgo detector in the following 10 years.

1. Introduction

Gravitational waves (GW) are one of the most robust predictions of General Relativity and have generated a lot of interest. Their existence has been proposed by Einstein in 1916 and they have been confirmed through observations on the binary pulsar PSR 1913+16 discovered in 1974 by J. Taylor and R. Hulse.[1] Subsequent observations by J. Taylor and J. Weisberg have shown that the decay of the orbit matches perfectly with what is predicted via energy loss by gravitational radiation emission.[2] General Relativity predicts that accelerating masses can produce ripples in space-time which propagate at the speed of light. They carry energy away from the source as well as information about the source. Thanks to the extremely weak coupling with matter, GW can cross the universe undisturbed and hence are a probe of the regions where they are produced which is not accessible by the electromagnetic counterparts - if produced which is not always the case. Thus, the detection of the relic emission of GW supposed to have occurred during the inflation era[3] would provide a unique way of investigating the early ages of the Universe (only a few moments after the Big Bang) well before the decoupling of the photons with matter (300000 years after Big Bang) which is the domain of the cosmic microwave background[4] studies. In that sense GW search represents a new window on the universe and a unique way to test theories of inflation or cosmic strings.

The frequency range of the majority of astrophysically produced GW is below 10 kHz. The first ground based GW detectors were the resonant bar detectors, composed of a large test mass operating at room temperature The passing GW is supposed to excite the fundamental resonant frequency of the material (1.6 kHz for the first bars). The vibration is then converted into an electrical signal by a motion transducer. After the pioneering work of J. Weber in the 60's, lots of improvement to increase the sensitivity have been carried out. The best performing bar detectors are now cryogenic suspended in vacuum[5–8] but even if their sensitivity achievement is astrophysically interesting their frequency bandwidth remains limited around their resonant frequency while for many signals the frequency bandwidth is much larger. In the late 70's, an alternative design of GW detector based on laser interferometry was proposed to overcome this limitation. Several projects have been developed over the world starting in the 90's: the American project LIGO[9] has two 4 km long and one 2 km long arm-length detectors which are now taking data continuously at their nominal sensitivity. A German-English collaboration GEO[10] is commissioning a 600 m long interferometer while the Japanese 300 m long TAMA[11] detector is now being upgraded after a few years of operation. Finally, the French-Italian 3 km Virgo[12] detector is still under commissioning. In parallel to research and development (R&D) endeavors for the second generation of ground based interferometric detectors, a spatial interferometric detector project LISA[13] will play an important role to study the huge number of sources expected below 100 mHz and not accessible to the ground based interferometer detectors.

The GW amplitude generated by accelerating masses is so weak that only compact and relativistic bodies may emit enough energy to be detected by ground based detectors such as the Virgo detector. As a result, the detection of GW implies astrophysical events and conversely the observation of GW will provide information about the astrophysical sources probing, in an unique manner, the behavior of matter in high density and strong gravity regions. The radiation of GW is fundamentally different from electromagnetic waves spawned by the acceleration of electrical dipoles: for GW emission, the accelerated mass must have a quadrupole moment. That is why a perfectly spherically symmetric supernova cannot emit any GW. Besides, it is possible that some sources of GW do not emit electromagnetic radiation. This is however not always the case; supernovae emit electromagnetic radiation and neutrinos which can be detected by underground neutrino detectors like for the SN1987A.[14–16]

Catastrophic events such as the coalescence of binary compact objects, neutron star (NS) or black hole (BH), and the core collapse of massive old stars represent the most promising sources of GW detectable by the first generation of ground based detectors, but many other astrophysical events are suspected to emit GW; rapidly spinning neutron stars not perfectly symmetric around their rotation axis may emit GW at twice the neutron star spin frequency. Strong evidence of that phenomena has been brought by the observation of the maximum spin frequency (650Hz) of NS accreting matter in a low mass x-ray binary system which is well smaller than the NS break-up limit (1.5 kHz). In such a system the spin-up due to accretion is balanced by the loss of energy via GW radiation.[17] The amplitude of this potential source is very weak but radio observation may help indicating location, expected frequency and spin-down. The maximum frequency range of these GW sources is known not to exceed 1300 kHz.

Other sources of GW are expected: newly born rapidly rotation neutron exciting the frequencies of the quasi-normal modes during the first minutes are expected to emit damped sinusoidal waveforms.[18] Furthermore, in association with type II supernovae recent studies have shown that the oscillations of the proto-neutron star core excited hundreds of milliseconds after the bounce may emit a huge amount of gravitational radiation leading to possible detection well beyond the Galaxy boundaries.[19]

The coalescence phase of a compact binary system ends by the merger of the two-body system into a single object. In the case of BH of masses higher than 20 $M_{\odot}$ the signal from the merger and subsequent ring-down phase is expected to be significantly detectable in the frequency band of interferometric detectors and may be dominant compared to the inspiral phase.[20] Recent breakthrough studies in Numerical Relativity provide for the first time waveforms of the BH-BH merger and ring-down phases.[21–23] It's a matter of fact that the theoretical predictions on waveforms are more and more accurate.

It's now thought that the GRB astrophysical generators are also GW emitters such as the compact binary merger for the short GRB and type Ic core collapse

supernovae for the long GRB. Despite the fact that the exact mechanism of GRB emission remains to be understood and the cosmological distances of the majority of the GRB, targeted searches GRB-GW are carried out with the ground based detectors.

Another source of GW may be due to the formation of cusps in cosmic strings.[24] The accumulation of cosmic strings GW emission may give rise to a stochastic background which might be difficult to detect by the first generation of interferometric detector. However, they may produce bursts of gravitational radiation on top of the stochastic background which might be more promising.

Finally the cumulative effect of all the already mentioned GW produced relatively recently gives rise to a stochastic background. Another mechanism of stochastic background production is the relic gravitational waves emitted by the early universe, as already mentioned.

2. gravitational wave detection principles

Gravitational Waves (GW) can be viewed as ripples in the curvature of space-time. When a GW crosses a given region a perturbation of the Minkowski metric is present. This perturbation effect being of changing the distance between two points in the space-time or two masses on Earth. The effect of the GW is transverse to the direction of propagation and in the transverse plane the distance between two points will be affected differently by the two polarizations h_+ and $h_\times$ of the GW. Let us consider the simple case of a linear polarized GW of amplitude h_+ ($h_\times$ is null in that case), the distance L between two points are stretched by $\Delta L = \frac{h_+}{2} L$. At the same time, due to the quadrupole nature of GW, in the perpendicular direction of the line formed by the two points, the same distance L is contracted by $-\Delta L$. In the case of a GW with two polarizations, the distances are stretched and contracted similarly by each polarization but the axes of deformation of the two polarizations are orthogonal to each other.

The main problem to detect GW is their very small predicted amplitude. Even the most violent astrophysical event occurring in the vicinity of the Earth would not generate a perturbation larger than, let's say, 10^{-21}. That means that one needs to be able to measure length displacements with a better accuracy than 10^{-21} which corresponds in the Fourier frequency domain and for a signal of a millisecond to a sensitivity of $3 \times 10^{-23}/\sqrt{\mathrm{Hz}}$. Laser Michelson-like interferometry provides a means and is particularly well suited to the detection of GW as they have a quadrupole nature. However a table-top Michelson interferometer with a laser power of 20 W has a shot noise limited sensitivity of $\sim 10^{-17}/\sqrt{\mathrm{Hz}}$. The basic Michelson scheme must be modified to reach the required sensitivity: 3 orders of magnitude are gained with km-long arms. The arms contain Fabry-Perot cavity increasing by another factor 30 the optical path of the photons. And finally the laser power which would exit the detector and head back toward the laser source is recycled inside the interferometer (gain of a factor of $\sim \sqrt{50}$) thanks to a mirror placed between the laser source and

the beam splitter mirror. The second interest of this laser interferometry technique is the frequency response to a GW, which is larger than 20 kHz. That fits well the frequency domain of the known GW sources. However, different sources of noise will limit the sensitivity of the interferometers. They are of different types; the so-

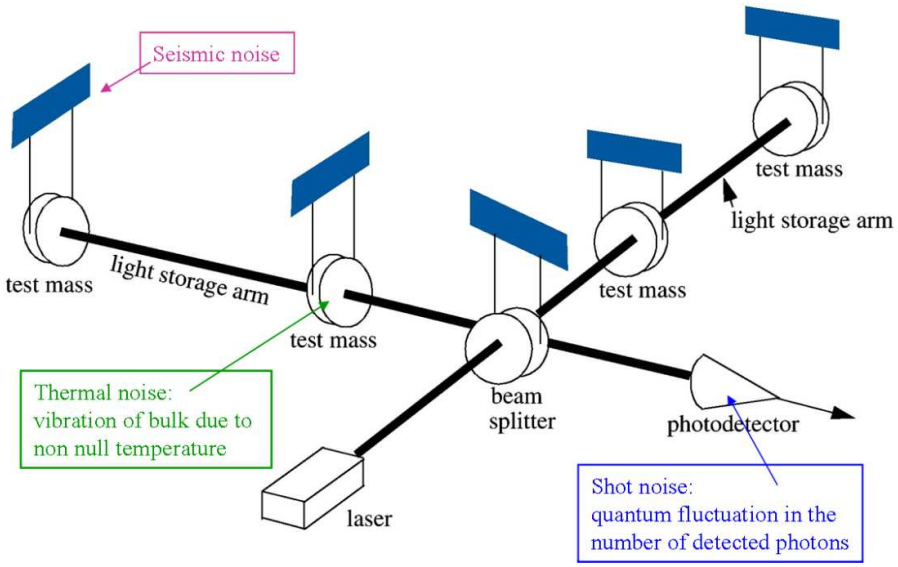

Fig. 1. A Michelson interferometer with Fabry-Perot cavities in the arms and the main fundamental noise sources. A passing GW will stretch one arm and contract the other. The mirrors are isolated from ground seismic noise above a few Hz thanks to the suspension system. But thermal noise in the substrate and in the wires will limit the sensitivity in the intermediate frequency domain. The sensitivity is limited at high frequency by the noise due to the photon counting statistics at the photo-detector output (shot noise).

called *fundamental* noise sources which will limit the sensitivity in absence of the other noise sources are the shot noise at high frequency, the thermal noise and the radiation pressure at lower frequency. The shot noise is due to the fluctuation of the measured signal (a number of photons collected on a photo-diode which follows a Poisson statistics). To reduce the shot noise, one needs to increase the laser power. But with high laser power, the radiation pressure fluctuation on the mirrors (due to the photon number fluctuation as well) can be high at low frequency if the test masses are not heavy enough. But given the laser power of the present ground based interferometers, the main limitation between a few tenth Hertz and a few hundred Hertz is the thermal noise of the mirrors and their wires due to the fact that the materials are at room temperature and to the friction between the materials composing the last suspension stage. It must be noted that another fundamental noise may limit the sensitivity below a few hundred Hertz is the gravity gradient

noise, due to the Newtonian coupling of the mirrors with the near-by masses which may fluctuate.

Before reaching the floor or these fundamental noises, one has to suppress the two other sources of noise; the seismic noise is part of the environmental and anthropogenic sources of noise. The solution is to suspend in vacuum all the optical components of the interferometer from a seismic attenuation system. Other environmental noise such as acoustic noise can induce displacement noise of critical optical components which must hence be enclosed in protected rooms.

Finally, the first source of noise that we must fight when commissioning the detector are the technical noises; actuator electronic noise, control system noise, laser power and frequency fluctuations and laser beam jitter have to be reduced such that at the end the sensitivity of the interferometer is dominated only by fundamental noises.

3. The Virgo detector and its commissioning

The Virgo[12] detector is a power recycled Michelson interferometer with 3 km long arms which each contain a Fabry-Perot cavity. All mirrors are suspended from the so-called Superattenuator which aims at reducing drastically above 10 Hz the seismic noise transferred to the instrument. In the following we describe the main components of the Virgo detector and the endeavors which have been carried out to control Virgo in its final configuration. At the end of 2005 a shutdown during two months was organized to fix problems which prevented Virgo from reaching its nominal sensitivity.

3.1. *Optical layout*

A simplified optical layout of the Virgo interferometer is shown in Fig. 2. A 20 W laser light @ 1064nm (delivering actually only 17 W) is provided by an injection-locked master-slave solid state 700 mW laser (Nd:YAG) located on the optical table (LB). The laser light is modulated in phase at a frequency of ~ 6 MHz (this technique permits the GW strain to be detected at the modulation frequency where the laser power fluctuation is much lower than in the interferometer bandwidth; this is the so-called frontal modulation technique). After passing the table (DT) which contains optics for the beam alignment, the laser light enters the vacuum system at the injection bench (IB) which is suspended. The beam is spatially filtered by a 144 m long input mode-cleaner triangular cavity (IMC) before being injected into the main interferometer. The laser frequency is pre-stabilized using the IMC cavity as a reference up to a frequency of 270 kHz. As the optical components of the IMC are suspended in vacuum this control provides a very good laser frequency control at high frequencies. The low-frequency stability is obtained by an additional control system that stabilizes the IMC length below 15 Hz to the length of a so-called reference cavity (RFC). The RFC is a 30 cm long rigid triangular cavity suspended in vacuum located beneath the IB; it consists of ULE, a material with a very low

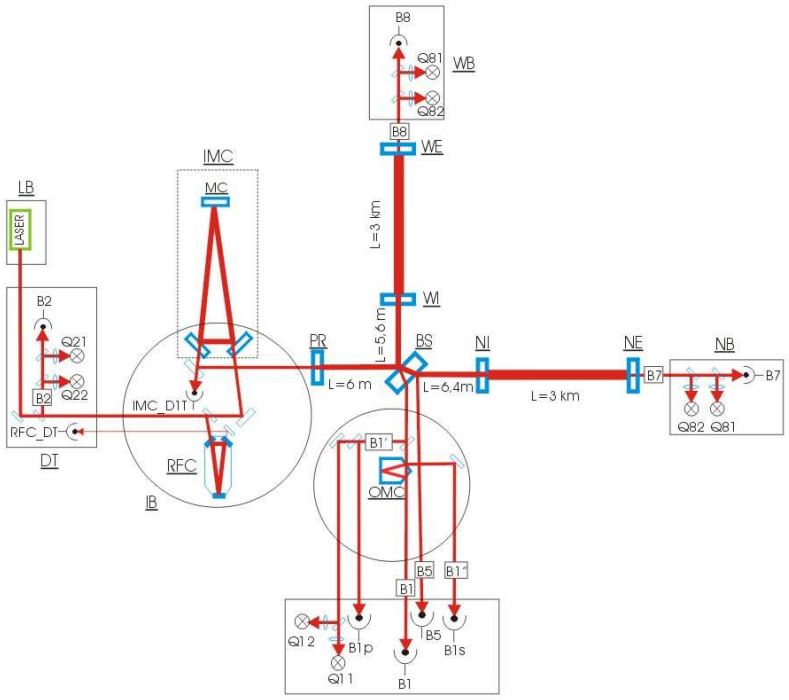

Fig. 2. The Virgo optical layout. The main optical components are drawn in blue. The photodiodes which are used for the longitudinal and angular control of the optical elements are represented on the different benches.

thermal expansion coefficient. This frequency pre-stabilization is mandatory to acquire the control of the different optical cavities, but to reach the extreme sensitivity targeted by Virgo an enhanced control of the laser frequency noise is required; the typical frequency noise of the principal laser source is given with $1\,\mathrm{kHz}/\sqrt{\mathrm{Hz}}$ at 10 Hz. In order to reach the desired sensitivity of Virgo this frequency noise has to be reduced to $3 \times 10^{-5}\,\mathrm{Hz}/\sqrt{\mathrm{Hz}}$.[25] This is the role of the so-called *second stage frequency stabilization* (SSFS) which is engaged during the cavities locking acquisition (see Section 3.2).

A 7 W power beam enters the Michelson interferometer through the power-recycling mirror (PR). It is then split by the beam splitter mirror (BS) into two beams that are injected into the 3 km long arm cavities. The Michelson interferometer is held on the dark fringe (destructive interference) in order to have a better contrast (apart from the mirrors' losses all light fed-in by the injection system returns to it). The PR mirror, with a reflectivity of 95%, reflects back the out-going light to the main interferometer. Together with the Michelson interferometer the power-recycling mirror forms a Fabry-Perot-like cavity in which the light power is resonantly enhanced. The recycling optical gain of this cavity is $\sim$ 40, which leads to 280W of light impinging the beam splitter. The finesse of the arm cavities has been measured to be close to 50. The Michelson interferometer is held on the dark fringe, and the GW strain signal is expected in the beam from the dark port, which

is leaving the vacuum via the so-called detection bench (DB). The detection bench is a suspended optical bench accommodating several optical components. The beam coming from the BS mirror passes through an output mode-cleaner (OMC), a 2.5 cm long rigid cavity. To achieve shot noise limited sensitivity, the main output beam is detected by a group of 16 InGaAs photodiodes. Actually only 2 photodiodes are in use now. For control purposes, other photodiodes are also used. Useful signals are obtained by detecting the light in the transmission of the arm cavities and in reflection of the power-recycling cavity, as well as detecting the reflection at the secondary surface of the beam splitter and the light reflected by the OMC. The GW signal that results from a detuning of the carrier resonance in the arms is extracted from the dark fringe channel demodulated and sampled at 20 kHz.

3.2. *Virgo control commissioning*

During 2 years starting in 2001, in parallel with the completion of the civil engineering work for the arms, the commissioning of the central part of the detector has provided a lot of experimental knowledge on the control of Virgo. The commissioning of Virgo in its final configuration commenced in mid 2003, and has been performed in several steps of increasing complexity: first individual Fabry-Perot cavities in the two arms have been controlled, then the implementation of a recombined Michelson Fabry-Perot interferometer has been an intermediate achievement before the final recycled Michelson Fabry-Perot interferometer control was achieved for the first time at the end of 2004.

The control of the interferometer consists in maintaining the laser light resonant in the optical cavities and the output port tuned on the dark fringe, defining its working point. More precisely, the carrier must be resonant in all cavities while the sidebands must be resonant in the central cavity but anti-resonant in the arms. Despite the good seismic noise attenuation provided by the Superattenuator, feedback controls are mandatory to maintain the interferometer locked on the right working point. But firstly, one needs to bring the interferometer from an uncontrolled condition to its working point by closing the different feedback loops; this is the so-called lock acquisition phase. The Fabry-Perot cavity locking scheme is based on the Pound-Drever-Hall technique[26] using reflected or transmitted demodulated signal. Four coupled lengths have to be controlled. This is managed sequentially by the Virgo Global Control system[27] which computes corrections that are sent to the different reference masses. Previously, the mirrors' speed has been calmed down (below 0.5 $\mu m/s$) thanks to the Local Control (LC) systems.[28] Initially a locking acquisition scheme based on LIGO's technique, has been tested. Unfortunately the control was quite unstable due to a strong dependence of the error signals on the interferometer's losses. Another technique has then been developed which gave encouraging results.[29] This technique called *Variable Finesse*[a] consists in locking the

[a]because the finesse of the recycling cavity is changed during the lock acquisition path.

cavities outside the working point for the dark fringe. In this way the recycling factor is low as a large fraction of the light escapes through the output port, resulting in less power in the interferometer. Then the interferometer is brought adiabatically on the dark fringe.

At this stage of the lock acquisition sequence an additional feedback control loop of the laser frequency noise is engaged. Indeed, due to the arms' asymmetry the laser frequency noise fluctuation is directly coupled with the differential mode of the interferometer (arms' length difference which contains the GW signal). A good reference signal to stabilize the laser frequency is actually provided by the long arm cavities of Virgo themselves whose lengths are supposed to be controlled with a relative accuracy better than $3 \times 10^{-20}/\sqrt{\mathrm{Hz}}$ at 10 Hz. The laser frequency pre-stabilization, described in Section 3.1, is slightly modified such that the IMC length is now locked on the length of the two arms cavities (common mode) with a 1 kHz bandwidth. This second stage frequency stabilization (SSFS) can only be engaged once the cavities are locked. The SSFS was implemented in a preliminary configuration in early 2004. Several improvements have been done so far and the system is now working reliably. The noise is below the requirements such that the Virgo sensitivity at high frequency is dominated by shot noise.

Another fundamental feedback control system concerns the alignment of the mirrors of the cavities with respect to each other and the alignment of all the optics with respect to the incoming beam. If uncontrolled, the angular degrees of freedom of the suspended optics distort the cavity eigen-modes. This causes power modulation of the light fields; furthermore, long term drifts will make the longitudinal control impossible after a certain amount time, and mis-alignments increase the coupling of other noise sources into the dark port (see Section 5). To guarantee a stable long-term operation and a high sensitivity the angular degrees of freedom have to be actively controlled using a low noise system (the LC controls the angular degrees of freedom but are too noisy). The Anderson technique for measuring and correcting the misalignment of optical components has been adapted to Virgo;[30] the laser light is modulated in phase at a specific RF frequency, such that the sidebands in the first order transverse modes (TEM_{01}) are resonant in the arm cavities. The transmitted light picked-up at four locations shown in Fig. 2 is detected by split photo detectors, namely quadrant photodiodes (QD) with four independent segments. The photo currents of these two QDs are demodulated at the RF frequency to yield signals proportional to the misalignment of the optical components. The auto-alignment system (AA) controls the two angular degrees of freedom (dof) Θ_x (rotation around the horizontal axis perpendicular to the beam) and Θ_y (rotation around the vertical axis) of the six main mirrors (PR, BS, NI, NE, WI, WE) and the injection bench (IB) using $4 \times 2 \times 2$ error signals for each dof. The relation between the tilts of the mirrors with the QD signals is expressed in a 16×7 matrix which can be measured once the cavity longitudinal dof are closed. A χ^2 based inversion of the optical matrix yields the correction signals which are finally fed back to the coils of the marionette. The LC servo loops are then progressively opened as soon as soon as

an AA loop is closed.

After having demonstrated in 2004 with one Fabry-Perot cavity that the Anderson technique works well, the 14 angular dof have been progressively closed; one of the difficulties encountered was the slow drift of the mirror positions which could not be cured with the LC (1-2 μ m per hour). To cope with that problem a slow drift control system with a bandwidth of a few mHz has been developed. In August 2005, 10 out of 14 angular dof loops have been closed with only one mirror and the IB remaining under LC[b]. As expected, the presence of the alignment control reduces the power fluctuations in the cavity considerably and allows long continuous operation as illustrated in Fig. 3 for the north arm cavity.

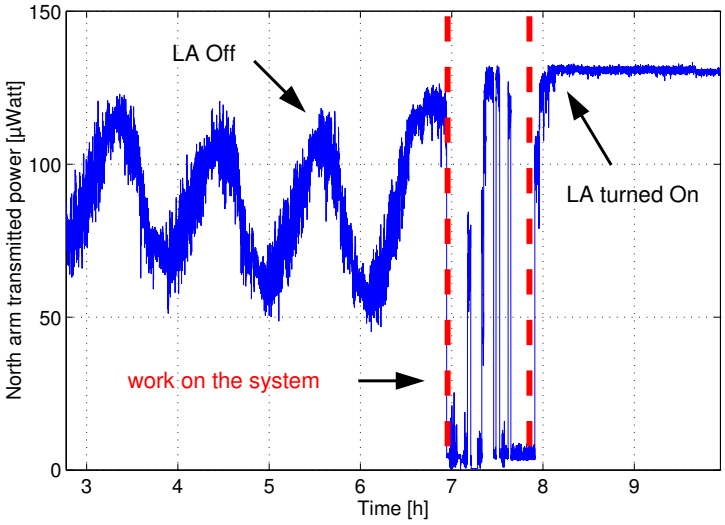

Fig. 3. Light power transmitted by the north arm cavity as a function of time before engaging the angular control (LA off) and after (LA turned on). The power fluctuations are strongly reduced.

The final steps of the Virgo locking acquisition procedure consist in locking the output mode-cleaner (OMC) whose main role is to suppress all high order TEM modes which can escape through the output port due to many reasons: asymmetries, mirror surface deformation, misalignments and mirror radius of curvature mismatch. The OMC is a short triangular monolithic cavity (3.6 cm) made of silica accommodated on the detection bench (DB) (see Fig. 2). This cavity is locked via a thermal control (the Peltier cell is connected to its support) changing the length of the cavity with a piezoelectric actuator. Once locked, the contrast on the output port is improved by a factor 10. The OMC is now used permanently and its lock is quite robust. An auto-alignment system using two QDs to center the beam

[b]The two remaining dof have been successfully closed after the time of this conference.

coming from the BS on the OMC has been developed. Finally, the last action is to re-allocate the force applied on the mirror to the two other stages of the Superattenuator in order to decrease the noise introduced by the actuators; this is the so-called *hierarchical control* which is described in Section 3.3.

Several short periods (from a few days up to 2 weeks) have been dedicated to data acquisition with the Virgo interferometer controlled in stable conditions. These seven commissioning runs allowed us to evaluate the progress achieved on the sensitivity curve once a major step in the full Virgo control was reached. The Virgo detector sensitivity progress achieved up to September 2005, just before the detector shutdown, are shown in Fig. 4. The two last runs (C6 and C7) correspond to the final recycled interferometer configuration, but running with only 0.7 W light power instead of 20 W as it will be explained in Section 4 (not all AA control loops were closed as well). Fig. 5 shows the contribution of several sources of noise which limited the sensitivity of the last commissioning run (C7). At low frequency (< 100 Hz) the longitudinal and angular controls of the mirror are the main limitation; the electronic noise of the actuator and/or the sensor introduced by the control loops induce a displacement of the mirror which is well above the fundamental noise floor which should be in that frequency region thermal noise. At higher frequency (> 300 Hz), the sensitivity was limited by the shot noise and the laser frequency noise.

3.3. *Virgo super-attenuation and hierarchical control*

While the Virgo detector uses an optical layout similar to that of other interferometric detectors, the main optical components are suspended from a sophisticated suspension system, the Superattenuator (SA)[31] in order to achieve a very high sensitivity down to low frequencies (> 10 Hz). This suspension system resides in up to 9 m tall vacuum chambers and is composed of six filter stages (see Fig. 6). The mirror and a reference mass each are suspended by two steel wires from a so-called marionette. Longitudinal forces to the mirror can be applied via coil-magnet actuators, with the magnets attached to the mirror surface and the coils being supported by the reference mass. In addition, coil-magnet actuators at the marionette level can be used to apply forces in longitudinal and angular directions. The topmost filter is rigidly connected to a ring that rests on three legs forming an inverted pendulum. This pendulum has a very low horizontal resonance frequency (40 mHz). While providing a good attenuation of seismic noise already at low frequencies, it also allows to move the top point of the suspension by up to ± 20 mm using very small forces.

At the resonance frequencies of the various isolation stages, the seismic motion is actually enhanced. Therefore, active controls are used to damp the mirror motion at these frequencies (from DC to approximately 5 Hz). The control is split into two parts, the inertial damping[32] (ID) and the local control[28] (LC). The ID is an active control system that uses three linear variable differential transformers (LVDTs) which measure a position with respect to the vacuum tank and three

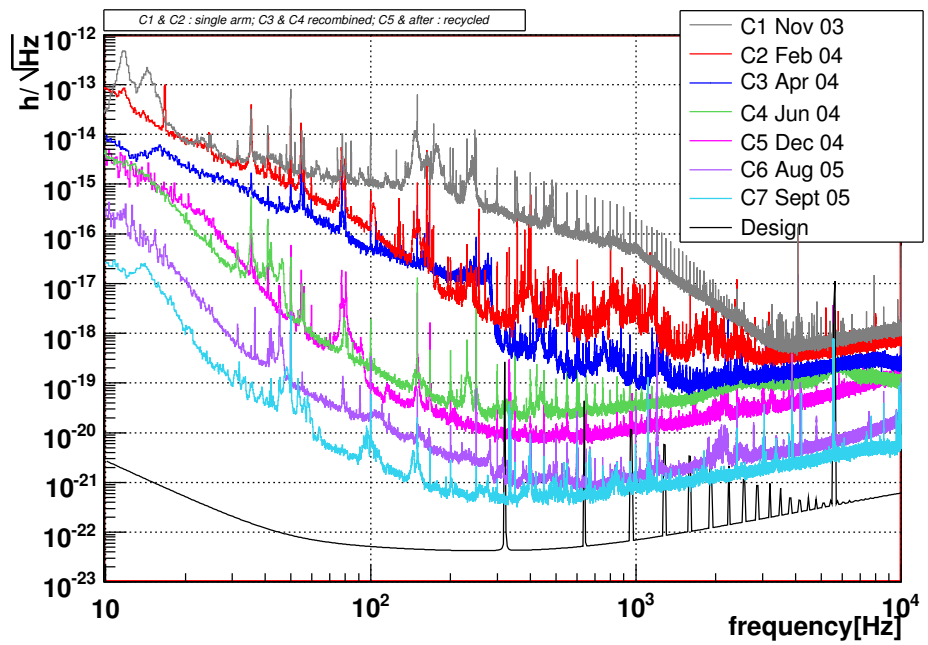

Fig. 4. Sensitivities curves obtained between 2003 and 2005 during the commissioning of the Virgo detector before the 2005 shutdown. The black curve is the Virgo nominal sensitivity curve which has been computed assuming a 10 W laser.

accelerometers located on the upper mechanical filter. Its main role is to freeze the SA motion between a few mHz and 2 Hz. The actuation is performed via three coil-magnet actuators also located on the topmost filter.

The LC can control the mirror in three degrees of freedom: the displacement along the optical axis (z), the angular rotation around the vertical axis (Θ_y), and the rotation around the horizontal axis perpendicular to the beam (Θ_x). The feedback for angular control is applied only via the coil-magnet actuators on the marionette, whereas longitudinal feedback can be sent to the marionette, to the reference mass actuators and to the top stage of the inverted pendulum.

The excellent passive seismic isolation of the Superattenuator has been characterized during the first phase of the Virgo commissioning.[33] Measurement of the seismic attenuation yielded a factor of 10^{-8} at 4Hz as an upper limit. The RMS motion of the mirror was measured to be below $1\,\mu$m and $1\,\mu$rad for longitudinal and angular displacement respectively when the ID control system is switched on, which is enough to acquire the lock of the cavities.

The Earth tides cause a slow regular elongation of the arm cavities of $\sim 200 \times 10^{-6}$ m amplitude (peak-to-peak). The dynamic range of the coil-magnet actuators at the mirror level (used for longitudinal feedback) is just $\sim 100 \times 10^{-6}$ m. To achieve

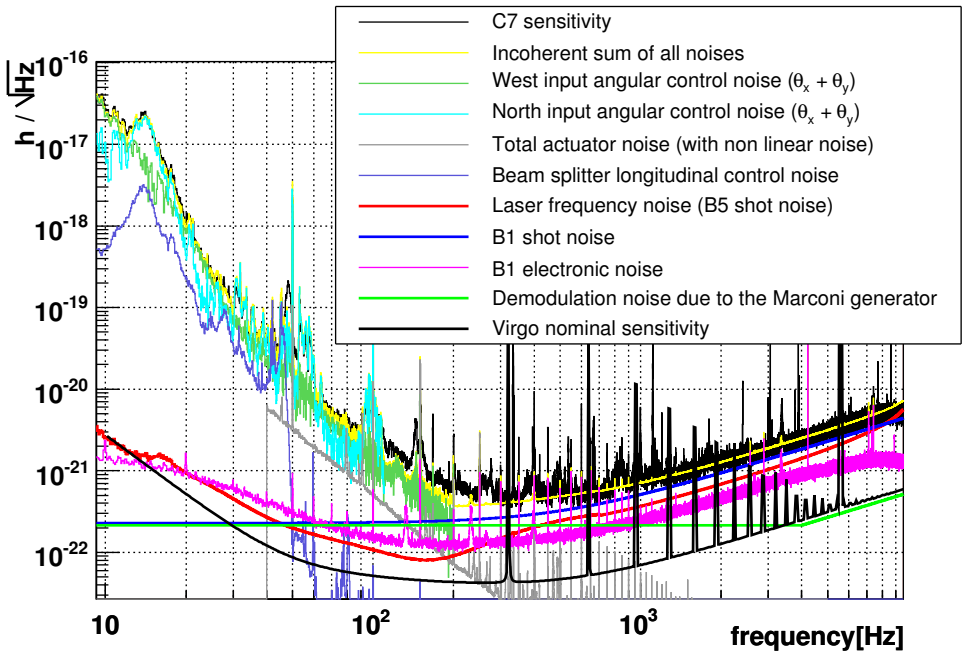

Fig. 5. Contribution of the different identified sources of noise which contribute to the sensitivity achieved by Virgo at the time of the C7 commissioning run (September 2005). The sensitivity was limited at low frequency by the noise re-introduced by the longitudinal and angular controls, while at high frequency ($>$ 300 Hz) the noise floor was limited half by the shot noise level and half by the laser frequency noise.

continuous stable operation one has to increase the dynamic range of the control. A hierarchical feedback system has been developed, which consists in sending low-frequency feedback (bandwidth 70 mHz) to the top stage of the suspension. Further reduction of the residual mirror motion can be achieved by acting at the level of the marionette below a few Hz. Thanks to this hierarchical control only nanometer residual mirror motion have to be compensate from the reference mass. The noise re-introduced by the electronics (mainly the DAC) is thus drastically reduced. It has been shown that this not only provides a compensation for the Earth tides but also reduces the RMS of the correction signals by one order of magnitude.[34]

4. Recent detector commissioning activities

In the fall 2005 a shutdown of the Virgo detector of 2 months was conducted to carry out important changes in order to cope with the limitations encountered during 2005. Indeed in 2005, Virgo was running with a reduced light power, 0.7 W instead of 10 W, because of the backscattering light in the mode-cleaner cavity reflected by the recycling mirror generating large amplitude fringes in the transmit-

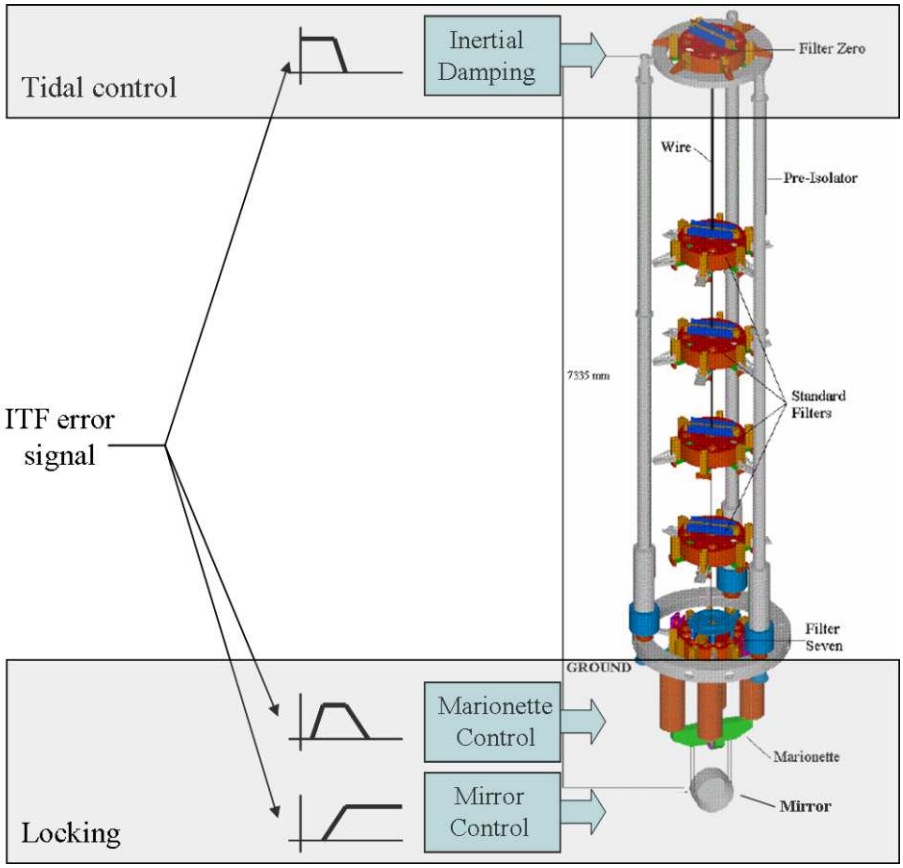

Fig. 6. The Virgo seismic attenuation system. It is composed of six filter stages hanged from an inverted pendulum forming a mixed passive and active attenuation system. The actuation points are indicated on the left.

ted IMC light power. As a result the laser frequency noise increased significantly which then created many difficulties to lock the different degrees of freedom of the interferometer. To fix that problem it was decided to install a Faraday isolator that can attenuate by a factor 10000 the backscattered light power.

The second major change concerned the replacement of the curved power recycling mirror. This mirror was composed of two block of Suprasil: in the center a curved mirror which was part of the output telescope to match the beam inside the interferometer is inserted inside an aluminum ring which is clamped to another block of Suprasil in order to have a heavy mirror. But this non-monolithic structure generated a lot of mechanical resonances not easily damped by the controls. The replacement with a flat and parallel face standard Suprasil mirror also makes the interferometer unaffected by the vertical position fluctuation of the PR mirror. On the other hand, it has been needed to implement all the telescope components on

the IB. Due to the very limited space left on this bench, a complete redesign has been carried out. We took advantage of this large modification to change the strategy of the IMC alignment with respect to the injected laser beam. In particular the RFC is now mounted after the IMC and a new beam alignment system (BMS) has been installed on the DT bench (see Fig. 2) which is independent from the RFC as before.

The installation of the new IB shown in Fig. 7 and the replacement of the PR mirror lasted 2 months such that in December 2005, the commissioning of the new injection system and of the Virgo detector could restart. The IMC has been relocked quite rapidly. On the contrary some difficulties have been encountered to lock the RFC as the procedure changed compared to the previous IB. A huge effort to align all optics on the bench has been carried out (it came out that many optical components were not aligned as expected). As soon as a stable beam could

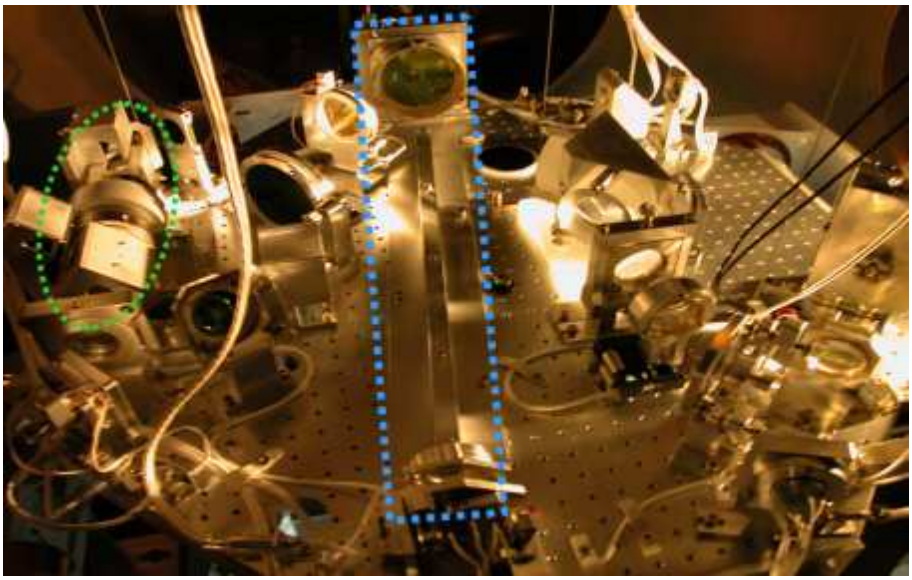

Fig. 7. The new Virgo injection bench installed at the end of 2005. The Faraday isolator is circled in green on the left. The new telescope is circled in blue in the middle of the bench.

be injected in the interferometer, its control was restarted, such that in April 2006 the recycled interferometer has been locked again. But the stability was very poor and the tuning of a few control systems was still pending (RFC auto-alignment, beam matching, parabolic telescope tuning, large beam astigmatism, global auto-alignment). All these IB fine-tunings required a few additional months of work and in July 2006 a beam matching of 95% has been achieved.

The optical isolation provided by the Faraday isolator has been measured to be a factor of the order of 100, while 10000 was expected. This did not prevent us

to work in good conditions with respect to the backscattering light issue. It has been understood later that the poor attenuation was due to a forgotten mounting key stuck to the permanent magnet of the Faraday isolator. The problem is now fixed. In parallel, the commissioning of the full interferometer restarted by especially improving the LC and the top-stage low frequency control to reduce the noise re-injected by these controls and the SSFS to reduce the laser frequency noise and increase its robustness. At the end of April 2006, 7 W was injected into the interferometer and 280 W was impinging the BS mirror, 10 times more than before the shutdown. Nevertheless, the lock of Virgo remained quite unstable (< 5 minutes) preventing the closing of the angular dof AA servo loops. One of the source of instabilities is due to thermal lensing effects in the mirror substrate due to the high power circulating now in the cavities.[35] It has been confirmed after the time of the conference that the sidebands in the recycling cavity (flat-flat cavity) are strongly affected by heating deformation of the substrates. At the end of 2006, the thermal effects remain a problem during the lock acquisition[c] although it does not prevent to acquire the lock and Virgo has been fully controlled with all AA loops closed. A thermal compensation system is now under study.

5. Virgo data analysis

The search for GW is organized in four working groups according to the main characteristics of the GW source: *burst* for all short duration GW, *inspiral* for the GW emitted during the coalescence of two compact objects, *pulsar* for the GW emitted by rotating asymmetric NS, and *stochastic* for the search of the residual stochastic background of GW. This later search can only be performed with another detector since the stochastic background must be observed coherently in pairs of detectors. In addition to these groups, an activity to identify the sources of noise and to understand and characterize the statistical properties of the Virgo data is done within the *noise* working group.[36]

In the last years, the sensitivity of the Virgo detector did not allow for competitive GW searches (the best NS-NS horizon[d] obtained so far is 1.5 Mpc). However the commissioning runs have been intensely used to settle the GW search pipelines facing real data issues. In particular, the last two commissioning runs C6 (14 days in July 2005 with a duty cycle of 90%) and C7 (5 days in September 2005 with a duty cycle of 65%) allowed the groups to discover many noise features in the Virgo data which complicate the GW searches. It should be remembered that the understanding of all fake GW found events is mandatory since they cannot be eliminated by performing coincidence analysis as it is currently done in the LIGO Science Collaboration[37] or the bar detectors.[38]

[c] the ten first minutes after the dark fringe working point is reached are sometimes critical and the interferometer control is lost.

[d] Here the horizon corresponds to the distance of detection of a NS-NS of 1.4 $M_\odot$ with a SNR of 8 assuming that the detector is optimally oriented.

Using the C7 data set, the *noise* group endeavors to identify and measure all the thin spectral features (lines) in the amplitude spectral density of the Virgo noise. This effort is particularly important for the pulsar search which consists in observing a permanent narrow line buried in the Virgo noise. Lines due to the environment (air conditioning system, vacuum pumps, electronic noisy boards, ...) and the rising thermal resonances of the mirrors and their wires have been identified. The *pulsar* group has done a blind search covering the frequency band 50-1050 Hz in the C6 and C7 data sets producing lists of candidates polluted by spurious events. They then performed a search for coincidences between the physical parameters (frequency, spin-down and sky position) of the two lists of candidates in order to reduce the false alarm probability.[39] In the *burst* group, one of the main activities since C5 run is to understand the origin of the detected candidate GW events, starting with those having the highest signal to noise ration (SNR). Actually the burst trigger rate for SNR>5 has been found to be 40 times higher than what one could expect from a Gaussian and stationary noise. A thorough investigation of the data allowed us to understand the origin of this excess of burst events due to a sporadic but important increase of the noise floor in a very large frequency band during from a few milliseconds up to a few seconds (see Fig. 8) . This noise increase corresponds to an increase of the coupling of the laser frequency noise with the dark fringe signal. The origin of the coupling fluctuation is due to large tilts of the mirrors whose angular dof are excited by some low frequency resonances of the SA (the AA control loops did not have enough gain at low frequency). This problem affecting about 25% of our data, were also a source of excess of fake GW events for the NS-NS binary searches performed by the *inspiral* group. This search is covering NS mass parameter between .9 and 3 $M_{\odot}$ for frequency between 80 Hz and 2 kHz. To eliminate the fake GW events, the burst and inspiral groups have started to design a veto procedure to suppress all the identified sources of noisy data periods.

In parallel to the individual Virgo GW searches, some collaborative efforts with other detectors are underway; burst and stochastic background searches in Virgo and the four Italian bar detectors have been tested on reduced data sets. However, burst, inspiral and stochastic background searches in a network of five interferometer composed of the LSC detectors and Virgo are more much promising. It has been shown that even with non perfectly aligned detector network, as LIGO-Virgo network, the burst and inspiral search performance is enhanced.[40,41] For the stochastic background, it has been shown that the pair GEO-Virgo has the best integrand sensitivity[e] for searches focusing on sources above 260 Hz due to the small distance between the two detectors, but *in fine* if one assumes a constant value of Ω_{GW} (the energy density of GW per unit of logarithmic frequency interval), the value which is favored by inflation and cosmic string models, the Virgo-GEO pair does perform similarly to the others above 300 Hz.

[e]this is a quantity which appears in the cross-correlation statistics which takes into account the overlap reduction function and the sensitivity of the detectors.

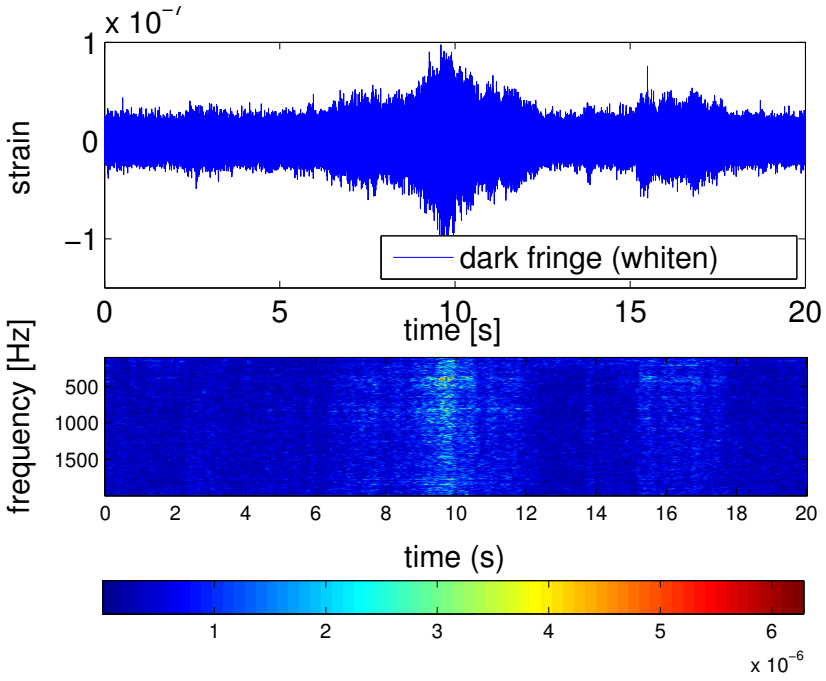

Fig. 8. Whitened Virgo strain amplitude (top) and spectrogram (bottom) for a 20 seconds period containing an increase of the noise floor that has been identified to be due to an enhancement of the laser frequency noise coupling due to the tilt of the north terminal building mirror.

6. Future Virgo upgrades

Assuming that the sensitivity reached by Virgo is limited by fundamental noises such as the thermal and shot noises, it will be of great importance to upgrade the detector in order to enhance its astrophysical sensitivity. A gain of a factor 10 in the sensitivity curve translates into an increase by a factor 1000 of the detection distance of potential GW sources. For that reason, the Virgo collaboration is now defining the path to a complete design of an advanced version of the detector.[42] The final design choice is foreseen at the end of 2007 and, if funded, *Advanced Virgo* will require many years of R&D.

In the meanwhile an intermediate upgrade program, *Virgo+*, is already planned. The shutdown should be relatively short because changes are compatible with the present Virgo optical configuration. The main explored paths to improve the sensitivity are the thermal noise and the shot noise reduction. To decrease the thermal noise, it is foreseen to replace the last stage of the suspension (marionette+wires+mirrors) with the so-called monolithic fused silica fiber suspension; this should reduce the friction noise and wire dissipation, and improve by a few orders of magnitude the quality factor of the pendulum mode of the suspension last stage. A full scale prototype installation is on-going on site in order to verify

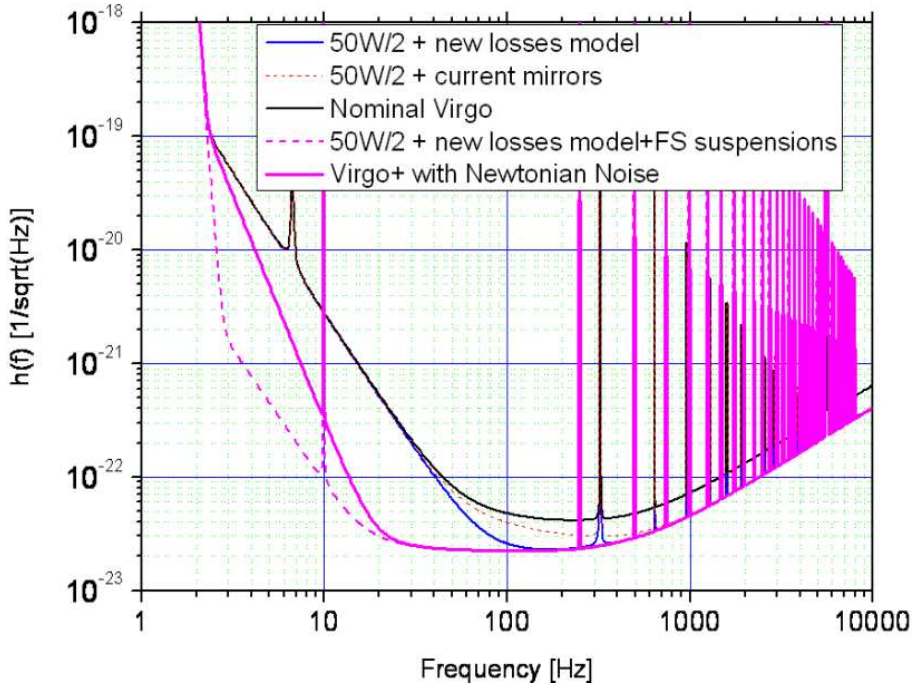

Fig. 9. Fundamental noise contributions of the expected sensitivity for Virgo after the *Virgo+* program upgrades. At low frequency pendulum thermal noise is expected to be reduced by at least one order of magnitude. The change of the Virgo mirrors material will improve the sensitivity above 100 Hz. The shot noise limit will be decreased thanks to the use of a 50 W power laser.

the engineering process and check the robustness of the monolithic suspension. The reduction of mechanical dissipation in the mirrors' coating will be critical as well and requires R&D. The input mirrors will be replaced with Suprasil 311 fused silica (very low losses). To reduce the shot-noise which dominates above a few hundred Hz one needs to increase the laser power. A 50 W power laser is foreseen to be installed.[43] Note that this laser power increase will require the change of many optical components. The Virgo control system is foreseen to be replaced (low noise electronics). The expected enhancement of the Virgo sensitivity is shown in Fig 9. In terms of GW discovery potential, *Virgo+* upgrades should increase the NS-NS horizon by a factor 3.5 up to 110 Mpc (optimal detector orientation).

7. Conclusion

Since the time of the conference, the sensitivity of Virgo has increased; in December 2006 the horizon is larger than 4 Mpc. However we still have one order of magnitude to gain in the 50-400 Hz region in order to reach the Virgo design sensitivity. A huge effort to hunt the different sources of noise limiting the sensitivity is ongoing in association with monthly week-end science runs in order to regularly test the

progress. Virgo is expected to reach its design sensitivity in mid 2007, which will then permit it to perform scientific sound GW searches in coincidence with the LIGO detectors before the shutdown foreseen for enhanced LIGO and Virgo+.

References

1. R. Hulse and J. Taylor, *Astrophys. J.* **195**, L51 (1975).
2. J. Taylor and J. Weisberg *Astrophys. J.* **345**, 434 (1989).
3. B. Allen, *Phys. Rev. D* **37**, 2078 (1988).
4. G. Smoot *et al*, *Astrophys. J.* **396**, 1 (1992).
5. http://www.roma1.infn.it/rog/explorer/explorer.html
6. http://gravity.phys.lsu.edu
7. http://www.lnf.infn.it/esperimenti/rog/NAUTILUS
8. http://www.auriga.lnl.infn.it
9. http://www.ligo.caltech.edu
10. http://www.geo600.uni-hannover.de
11. http://www.tamago.mtk.nao.ac.jp
12. http://www.virgo.infn.it
13. http://www.lisa.nasa.gov
14. K. Hirata *et al*, *Phys. Rev. Lett.* **58**, 1490 (1987); Phys. Rev. D **38**, 448 (1988).
15. Y. Fukuda *et al*, *Phys. Rev. Lett.* **81**, 1158 (1998).
16. J. Boger *et al*, *Nucl. Instrum. Methods Phys. Res. A* **449**, 172 (2000).
17. L. Bildsten, *Astrophys. J.* **501**, L89 (1998).
18. V. Ferrari, G. Miniutti and J. A. Pons, *Class. Quantum Grav.* **20**, S841 (2003).
19. C. Ott *et al*, *Phys. Rev. Lett.* **96**, 201102 (2006).
20. E. E. Flanagan and S. A. Hughes, Phys. Rev. D **57**, 4535 (1998).
21. J. Baker *et al*, Phys. Rev. D **73**, 104002 (2006).
22. F. Pretorius, Phys. Rev. Lett. **95**, 121101 (2005).
23. M. Campanelli *et al*, Phys. Rev. Lett. **96**, 111101 (2006).
24. T. Damour, A. Vilenkin, *Phys. Rev. Lett.* **85**, 3761 (2000).
25. M. Barsuglia, PhD thesis, Université Paris-Sud, LAL 99-25 (1999).
26. R. Drever *et al*, *Appl. Phys. B: Photophys. Laser Chem.* **31** 97 (1983).
27. N. Arnaud *et al*, *Nucl. Instrum. Methods Phys. Res. A* **550**, 467 (2005).
28. F. Acernese *et al.*, *Astrop. Phys.* **20** (6), 617 (2004).
29. F. Acernese *et al*, *Class. Quantum Grav.* **23**, S85 (2006).
30. D. Babusci *et al*, *Phys. Lett. A* **226** (1), 31 (1997).
31. G. Ballardin, *et al.*, *Rev. Sci. Instrum.* **79** 9, 3643 (2001).
32. G. Losurdo, *et al.*, *Rev. Sci. Instrum.*, **79** 9, 3653 (2001).
33. F. Acernese, *et al.*, *Astrop. Phys.* **21** (1), 1 (2004).
34. F. Acernese, *et al.*, *Astrop. Phys.* **20** (6), 629 (2004).
35. M. Barsuglia for the Virgo collaboration, *this proceedings.*
36. E. Cuoco for the Virgo collaboration, *this proceedings.*
37. B. Abbott *et al*, *Phys. Rev. D* **72**, 062001 (2005).
38. P. Astone *et al*, *Phys. Rev. D* **68**, 022001 (2003).
39. C. Palomba for the Virgo collaboration, *this proceedings.*
40. F. Beauville *et al*, *submitted to Phys. Rev. D*, gr-qc/0701027
41. F. Beauville *et al*, *submitted to Phys. Rev. D*, gr-qc/0701026
42. R. Flaminio *et al*, "Advanced Virgo White Paper", VIR-NOT-DIR-1390-304
43. N. Man for the Virgo collaboration, *this proceedings.*